Removal of adsorbing estrogenic micropollutants by nanofiltration membranes

Removal of adsorbing estrogenic micropollutants by nanofiltration membranes. Part A - experimental evidence

Journal of Membrane Science
2013
Volume 431, 244-256

Andrea J. C. Semião*, Andrea I. Schäfer
School of Engineering, The University of Edinburgh,
Edinburgh, EH9 3JL, United Kingdom

* Corresponding author: Andrea J. C. Semião, Presently at University College Dublin, E-mail: Andrea.Correia-Semiao@ucd.ie, Phone: +353 (0) 17161974

Abstract

Nanofiltration membranes should be effective in removing hormones based on hormone molecular size. However, the occurrence of adsorption onto the membranes results in a lower performance than would be expected by size exclusion. It is hence important to understand the retention mechanisms involved in the removal of adsorbing trace contaminants.

The focus of this study was to elucidate how estrone and estradiol adsorption and retention are affected by intrinsic membrane characteristics such as different polymeric materials and membrane pore radius.

Polyamide raw material and polyamide active layer of TFC NF membranes were found to adsorb much higher amounts of hormones than any of the other membrane materials that constitute the membranes, i.e. polysulfone and polyester. These results show that the bulk of the adsorption occurs in the active layer. The adsorption isotherm onto the different raw polymeric materials was found to be of the Freundlich type, and interactions between hormones and the different polymers can be explained by H-bonding and weak π- π interactions, amongst other interactions, and not hydrophobic interactions.

Adsorption and retention were further found to be affected by the membrane active layer pore size, hence the steric exclusion capacity of the membrane, which dictates how much hormone partitions into the membrane pores. An increase of pore radius from 0.32 nm to 0.52 nm increased the amount of hormone that partitions into the membrane pores, thus affecting adsorption, which increased from 0.17 ng.cm^{-2} to 1.10 ng.cm^{-2}. Retention, on the other hand, decreased from 88% to 34%.

Finally, hormones were shown to penetrate and adsorb inside the active layer at pH 7, whilst at pH 11, adsorption was confined to the membrane surface due to electrostatic repulsion. The membrane internal surface area of the active layer played a role in adsorption. At neutral pH, the more internal surface area the membrane had, the more adsorption took place. There is therefore a combination of partitioning effect and internal surface area access playing a role in hormone adsorption and retention by NF membranes.

Keywords: Adsorption, estrogens, pore radius, material affinity, internal surface area.

1 Introduction

Trace organics, including hormones, pesticides and personal care products are discharged into surface waters from the $ng.L^{-1}$ up to the $\mu g.L^{-1}$ concentration [1]. Since they pose an environmental risk to organisms and in consequence, possibly to human health, [2], they should be removed from natural and potable water sources.

Nanofiltration (NF) is a possible application for water treatment. Removal of adsorbing trace organics by NF membranes is however not well understood. It has been well established that adsorbing trace contaminants have a lower retention than would be expected by size exclusion [3]. This is thought to be caused by the partitioning of trace organics onto the polyamide active layer [4]. No link has however yet been established between adsorption of trace contaminants and the membrane characteristics (*e.g.* pore size, solute-membrane affinity). The parameters affecting adsorption and transport of trace contaminants by NF membranes need therefore to be elucidated.

Understanding transport of adsorbing compounds through NF membranes in filtration mode requires the knowledge of the mechanisms and physical parameters governing the process. It was previously found that the concentration at the membrane surface governs hormone adsorption onto NF membranes [5]. The membrane was, however, treated as a black box and no membrane characteristics were included in the study. Determining such mechanisms and physical parameters as far as membrane characteristics are concerned (*e.g.* pore radius, membrane materials) is therefore a necessary next step.

Adsorption of trace contaminants onto different types of polymeric membranes has been extensively reported in the literature [6]. Polyamide based membranes, for example, have been shown to adsorb more trace contaminants than cellulose acetate ones [7]. Other polymeric materials such as polypropylene and polyimide have shown to adsorb trace contaminants [8, 9]. The adsorption of trace contaminants onto NF polymeric membranes have been proposed to be either caused by charge interactions [10], hydrophobic interactions [11] or hydrogen-bonding interactions [12]. Other mechanisms such as dipole-dipole, induced dipole-dipole interactions might also affect the interaction between the contaminant and the membrane [6]. However, for the particular case of hormones, when comparing the amount adsorbed with their chemical properties for the NF270 [6], electrostatic repulsion, hydrophobicity and dipole moment do not explain the differences in sorption obtained for the several hormones.

Thin film composite (TFC) NF and RO membranes are made of three different polymeric layers and to understand and model the removal of adsorbing trace contaminants it is necessary to determine in which layer(s) adsorption occurs onto.

Several authors have carried out static adsorption experiments with membrane coupons of the polysulfone (PSu) support with and without the polyamide (PA) active layer. Williams *et al.* [13] and Steinle-Darling *et al.* [14] obtained much higher adsorption of phenolic compounds and perfluorochemicals, respectively, onto PA+PSu compared to just PSu. McCallum *et al.* [15] results showed that hormone adsorption onto PA+PSu was slightly higher than PSu only. Polyester (PET), the third material of TFC membranes, was shown not to adsorb any hormones. These results give a good indication of the affinity of the contaminant with the different materials. However, it is difficult to determine the affinity of the contaminant for each material independently. The affinity with PA is carried out in the presence of PSu since these two layers are not possible to separate and competition between the two layers might occur. A systematic study for the separate polymers is therefore necessary to properly establish the differences in affinity between the hormone and the polymeric materials.

The effect of pore radius on trace contaminant adsorption and retention by NF membranes is important since it allows determining if steric exclusion (*i.e.* solute to pore radius ratio) needs to be taken into account when modelling adsorption onto NF membranes. In general, retention increases with increase of compound molecular weight [16] showing a size exclusion mechanism. Nghiem *et al.* [17] however, showed that adsorbing hormones have a lower retention than would be expected if only steric interactions were considered. Furthermore, hormone adsorption was found to be higher for two NF membranes compared to an RO membrane, suggesting a pore radius effect in hormone adsorption and retention by polymeric membranes [12].

Several studies [18, 19] have suggested the occurrence of internal adsorption of trace contaminants on the NF active layer. Kimura *et al.* [20] obtained lower contaminant extraction in static mode from membranes saturated under pressure (40-60%) compared to membranes saturated under static conditions (100%). McCallum *et al.* [15] on the other hand obtained 100% extraction efficiency when carrying out the desorption under pressure of a pre-saturated membrane. All these studies indicate that membrane adsorption occurs inside the active layer. If this is the case, then pore radius could not be the only parameter affecting adsorption and retention of trace contaminants by NF membranes: internal surface area may play an important role as well. In consequence, a systematic study to determine the contribution of internal surface area is required.

In our previous review [6] preliminary experiments indicated an effect of pore radius and internal surface area on the adsorption of hormones in NF membranes and showed there was a difference between the hormone adsorption onto one weight of the different raw polymers. A more in depth study on the effect of these different parameters in adsorption of trace contaminants in NF membranes was however needed.

In the present study the relevant membrane characteristics needed to understand and model transport of adsorbing hormones through NF membranes were systematically determined, extending the preliminary work showed in the review by Schäfer *et al.* [6]. Understanding how these parameters, such as pore radius and internal surface area, affect adsorption and retention of hormones by NF membranes is a first step as it allows deciding which approach is the most appropriate to model transport of adsorbing hormones through NF membranes.

The affinity of the hormones onto the different raw materials that constitute TFC membranes was established, as well as the isotherm and its parameters. The adsorption of hormones onto the polyamide and polysulfone layers of the NF 270 membrane was further quantified. Several TFC NF membranes were then characterised in terms of pore radius and active layer thickness to porosity ratio. This allowed to study the effect that pore radius has in hormone adsorption and retention. Moreover, the effect of the active layer internal surface area in hormone adsorption was considered in this study. Finally, the occurrence of internal sorption on the active layer was showed by carrying out desorption experiments of pre-saturated membranes under pressure.

2 Materials and Methods

2.1. Filtration Set-up

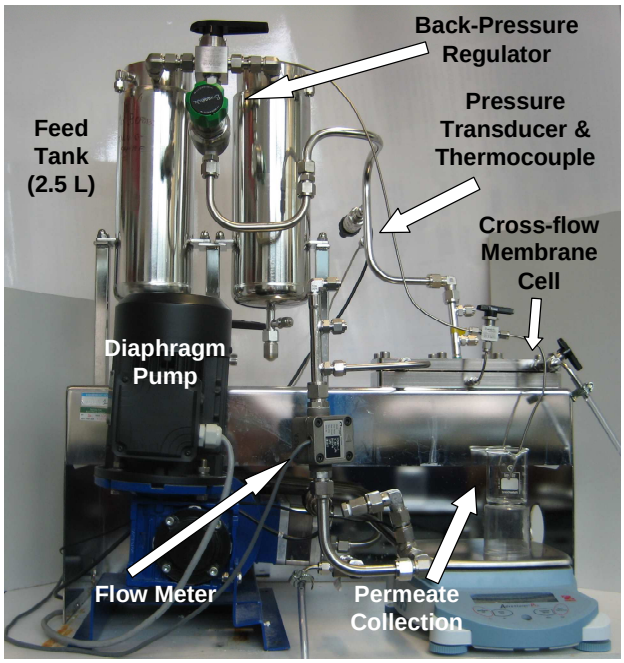

Figure 1 Cross-flow filtration set-up

A stainless steel cross-flow system (Figure 1) used for the filtration experiments, has been described elsewhere [6]. The system is connected to a flat sheet membrane cell (MMS, Switzerland)

of 46 cm^2 surface area, with a slit type channel height of 1.10^{-3} m, width of 0.025 m and length of 0.191 m. The permeate mass was measured using a Ohaus Adventurer Pro electronic balance (Leicester, UK).

2.2. Membranes and membrane characterisation

Several TFC membranes were used in this study: BW30, NF90 and NF270 (Dow Filmtec), two batches of TFC-SR2 and TFC-SR3 (Koch membranes). The membranes permeability and NaCl retention are presented in Table 1.

The membranes roughness R_A was measured by AFM (Bruker Corporation, USA) with a cantilever Micromask CSC38/AIBS-B. This cantilever uses a resonance frequency of 10 kHz and has a spring constant of 0.03 $N.m^{-1}$. The measurements were carried out with contact mode in liquid (MilliQ water) and a scan size of 2.0 x 2.0 µm.

Table 1 Membrane Characteristics

Membrane Type	**Permeability ($L.h^{-1}.m^{-2}.bar^{-1}$)**	**NaCl Retention (%) (0.1 M, 10 bar)**	**Roughness R_A (nm)**	**Streaming Potential at pH 11 (mV)**	**Average Active Layer Thickness (nm)**	**Average Active Layer Thickness in Literature (nm)**
BW30	4.1 ± 0.3	99.8	67.7 ± 2.4	-20	233 ± 88 [21]	-
NF90	10.6 ± 1.6	88.7	61.7 ± 2.1	-15 [22]	218 ± 40	[23]
TFC-SR2 1	12.5± 2.3	22.3	17.9 ± 0.6		345 ± 28	-
TFC-SR2 2	7.2 ± 0.6	23.4	17.9 ± 0.6	-25	345 ± 28	-
TFC-SR3	6.7 ± 0.8	40.8	5.2 ± 0.6	-25	400 ± 10	-
NF 270	17.0 ± 0.8	52.0	4.2 ± 0.3	-25	21 ± 2.4	[24, 25]

The active layer thicknesses were obtained from TEM measurements for the TFC-SR2 1 and 2, the NF 270 and the NF 90 membrane [26]. The BW30 thickness was obtained from the literature [21] and since no results are reported in the literature for the TFC-SR3, a thickness of 400 nm (maximum thickness reported for NF membranes) was assumed. References from the literature for the NF 90 and NF 270 membranes are provided in Table 1 for similar values obtained for the average active layer thickness.

The active layer thicknesses and thickness variability were determined from the TEM pictures with Image J (version 1.40). It was noticed from Table 1, that the variability obtained in the membrane thickness from the TEM images correlates with the roughness of the active layer. Since

there are no images available for the TFC-SR3 thickness, a variability of 10 nm was assumed, using a similar value as the one obtained for its roughness.

Streaming potential of flat sheet nanofiltration membranes was measured using the electrokinetic analyser EKA, (Anton Paar KG, Gratz, Austria) with an electrolyte solution of 20 mM NaCl, and 1 mM $NaHCO_3$. The streaming potential result for NF 90 was found in the literature and measured for the same conditions.

The membranes were all characterised for pore radius and active layer thickness to porosity ratio with several inert organics. The BW30, NF90, TFC-SR2 1 and 2 and NF270 characterisation was done in the cross-flow system at different pressures (Q_{feed}=2 $L.min^{-1}$ to avoid polarisation, T=24°C). The system ran for 1 hour at each pressure, and a feed and permeate sample of 15 mL was collected for analysis in a TOC V_{CPH} (Shimadzu, UK) in the NPOC mode with the high sensitivity catalyst. The TFC-SR3 characteristics were published elsewhere [27].

2.3. Chemicals and Reagents

The radiolabelled hormones used were [2,4,6,7-^{3}H] estrone (E1) and [2,4,6,7-^{3}H] 17β-estradiol (E2) (Perkin Elmer and GE Healthcare, UK). An initial hormone feed concentration of 100 $ng.L^{-1}$ was used in all the experiments, unless otherwise stated. 0.5 mL of sample was placed in a scintillation vial (Perkin Elmer, UK) with 4 mL of Ultima Gold LLT (Perkin Elmer, UK) and counted for 10 minutes each using a Beckman LS 6500 scintillation counter (Fullerton, USA). The detection limit of this method is 1 $ng.L^{-1}$ ± 2% for the hormones studied.

All chemicals were of analytical grade and were purchased from Fisher Scientific (Loughborough, UK): 1 M NaOH was used for pH adjustment, pure acetone was used for hormone desorption and 0.1 M of NaCl was used for the membrane characterization. Several organics at 25 $mgC.L^{-1}$ of feed concentration in MilliQ water were used for the membrane characterization: dioxane, dextrose (Fisher Scientific, UK) and xylose (Acros Organics, UK) were used for all the membranes. Methanol (Fisher Scientific, UK), which has a low molecular weight, was further used for the BW30 membrane as this membrane is very tight.

Several raw polymers that constitute the TFC NF membranes were used to study their adsorption capacity of hormones: polyamide (PA), polyethylene teraphtalate (PET), polyethylene naphtalate (PEN) and polysulphone (PSu). These were purchased from Goodfellow (Huntingdon, UK) in the form of 2 to 3 mm granules and polysulphone (PSu) was kindly offered from Solvay (Brussels, Belgium) in granular form. Their properties are presented in Table 2.

Polymers were grinded to a size smaller than 500 μm with a Retsch Ultra Centrifugal Mill ZM 200 (Leeds, UK), in three stages using sieves with 1000, 750 and 500 μm openings. The

grinded polymer surface area was determined by electron microscopy and analysed with the software ImageJ (version 1.40), assuming that particles have a spherical shape.

Table 2 Polymer type, abbreviation (Abbr.), supplier, and selected characteristics for polymer powders used in adsorption studies: monomer molecular weight (MW) and contact angle (CA)

Polymer	**Abbr.**	**Supplier**	**Structure**	**Monomer MW (g/mol)**	**CA (º)**
Polysulphone	PSu	Solvay	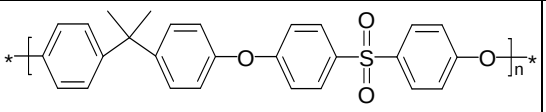	442	84 [28]
Polyester: Polyethylene Teraphthalate	PET	Goodfellow	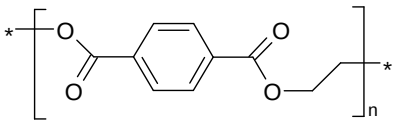	192	81 [29]
Polyester: Polyethylene Naphthalate	PEN	Goodfellow	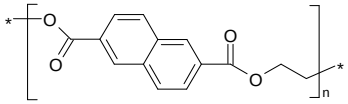	242	80 [30]
Polyamide: Nylon, 6	PA	Goodfellow	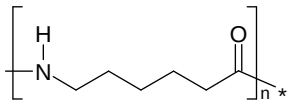	113	70 [29]

2.4. Hormone Static Adsorption onto Polymeric Materials and TFC NF membranes

Grinded polymer masses from 0.25 g to 3.1 g were placed in 60 mL of a solution containing 100 $ng.L^{-1}$ E2 and shaked in a Certomat BS-1 UHK-25 shaker (Göttingen, Germany) at 200 rpm and 25ºC. Samples were regularly taken, filtered with 0.7 μm glass microfibre filters (Fisher Scientific, UK) placed in Millipore Swinnex filter (Ireland) support and counted. The hormone mass adsorbed on the polymer was then obtained by mass balance.

Hormone static adsorption onto the different NF membranes was carried out. A membrane area of 2 cm^2 was gently washed with MilliQ water, placed in 60 mL of E2 solutions of different concentrations (25, 50, 100 and 200 $ng.L^{-1}$) and shaken for at least 48 hours at 200 rpm and 25ºC.

2.5. Hormone Adsorption on the PA and PSu layers of a TFC Membrane

A diffusion cell was used to measure the adsorption of hormones on the NF 270 membrane PA_m and PSu_m surfaces separately.

The membrane was gently washed with MilliQ water and PA_m+PSu_m was physically peeled from PE_m. The PA_m+PSu_m was then cut to 40 mm of diameter and placed in a diffusion cell of 25 mm diameter. The membrane area exposed to the solution on each side is 4.9 cm^2. The diffusion cell is made of glass and has two cells of 150 mL volume each which are constantly stirred with a stirrer (Fisher Scientific, UK) at 1000 rpm. The membrane is placed between the two cells, tightened with clamps, with each side of the membrane facing a different cell.

A solution of 125 mL of hormone at a determined concentration is placed in both cells (*i.e.* cell facing the PA_m layer and the cell facing the PSu_m layer) for 8 hours: this was the amount of time determined in a previous experiment when water diffuses from the PSu_m cell and starts appearing on the PA_m cell. Concentrations of 100 $ng.L^{-1}$ for both hormones, 20 $ng.L^{-1}$ for E1 and 30 $ng.L^{-1}$ for E2 were placed in contact with PA_m and PSu_m to mimic filtration conditions [5]. Hormone samples were taken from both cells at regular intervals and measured in the scintillation counter. The amount adsorbed was obtained by mass balance to each feed cell.

2.6. Hormone Adsorption Filtration Protocol

The membrane coupon, washed and stored in MilliQ water for at least 12 hours, was placed in the cross-flow cell and compacted for two hours with MilliQ water at 25 bar. The pure water flux was measured at 25 bar for at least 30 minutes to ensure steady flux followed by flux measurement at the experimental pressure for ten minutes. The system was then emptied and replenished with 1.5 L of fresh MilliQ water, which is recirculated in the system for one hour at a set pressure (3 to 17 bar) and feed flow rate Q_{feed} (0.5 to 2 $L.min^{-1}$) to ensure all process parameters were constant.

A volume of 0.5 L of hormone solution was then added to the 1.5 L of circulating MilliQ water to reach the required hormone concentration in the system and mixed well using a mechanical stirrer at 200 rpm (Gallenkamp, UK). The feed and permeate hormone concentrations were measured at regular time intervals (every five minutes for the first half hour and then once every hour) to obtain the transient trend until equilibrium was reached (average of 8 hours). The transient mass adsorbed was then obtained by mass balance to the feed tank. A new membrane was used for every experiment.

2.7. Hormone Desorption from Saturated Membrane

Different desorption experiments of E1 from the NF 270 membrane were carried out:

- Static desorption from a 2×5 cm rectangle of cross-flow pre-saturated membranes at different pressures (from no pressure to 15 bar). The polyester (PE_m) bottom layer was physically separated from the top layers of polyamide and polysulfone (PA_m+PSu_m). These were placed separately in 25 mL of acetone in a Certomat BS-1 UHK-25 (Göttingen, Germany) incubator shaker at 200 rpm and 25ºC for at least 48 hours, when the hormone concentration was measured. Acetone was found to have no influence in the scintillation counting process.
- Static desorption experiments from pre-saturated membranes in static mode (no pressure). 15 mm of diameter of membrane pieces were placed in 60 mL of E1 solutions (50, 100 and 500 $ng.L^{-1}$) and left to adsorb in the shaker for at least 48 hours. Once saturation reached steady-state, the membrane pieces were removed from the solutions, left to dry for a few minutes and then placed back in the shaker in 10 mL acetone and left to desorb for at least 48 hours.
- Filtration desorption at 11 bar from a cross-flow pre-saturated membrane (C_{feed} E1=50 $ng.L^{-1}$, P=11 bar, Re_h=427). Filtration desorption was first carried out with MilliQ water then with 2% acetone solution.

3 Results and Discussion

3.1. Adsorption onto Different Polymeric Materials

Commercial TFC NF membranes are made of several polymeric materials: PA, PSu, PET and PEN. The first step in understanding adsorption of hormones onto TFC NF membranes is to establish which layer the hormones adsorb onto. In order to compare the affinity of E2 towards the different polymeric materials adsorption isotherms were determined as presented in Figure 2 A.

The isotherms convex upwards, indicating a Freundlich type isotherm (Figure 2 A). The Freundlich isotherm (equation 4) assumes several types of sorbing sites available on the surface, where each type possesses a different sorption-free energy and abundance.

$$M_{ads} = K_f C_{equilibrium}^{1/n_i} \quad (4)$$

where M_{ads} is the mass adsorbed per polymer surface area ($ng.m^{-2}$), K_f is the Freundlich capacity factor related to the adsorption capacity of the sorbent ($ng^{(1-1/ni)}.m^{(3/ni-2)}$), $C_{equilibrium}$ is the hormone

concentration in solution at equilibrium (ng.m^{-3}) and n_i is the Freundlich exponent, related to the energy of adsorption. The logarithmic form of equation (4) yields equation (5):

$$\mathrm{Log}(M_{ads}) = \frac{1}{n_i}\mathrm{Log}(C_{equilibrium}) + \log(K_f) \qquad (5)$$

To confirm if the isotherms are of the Freundlich type, the data in Figure 2 A is represented in logarithmic form (Figure 2 B) and the linear fitting provides the Freundlich coefficients K_f and n_i according to equation (5).

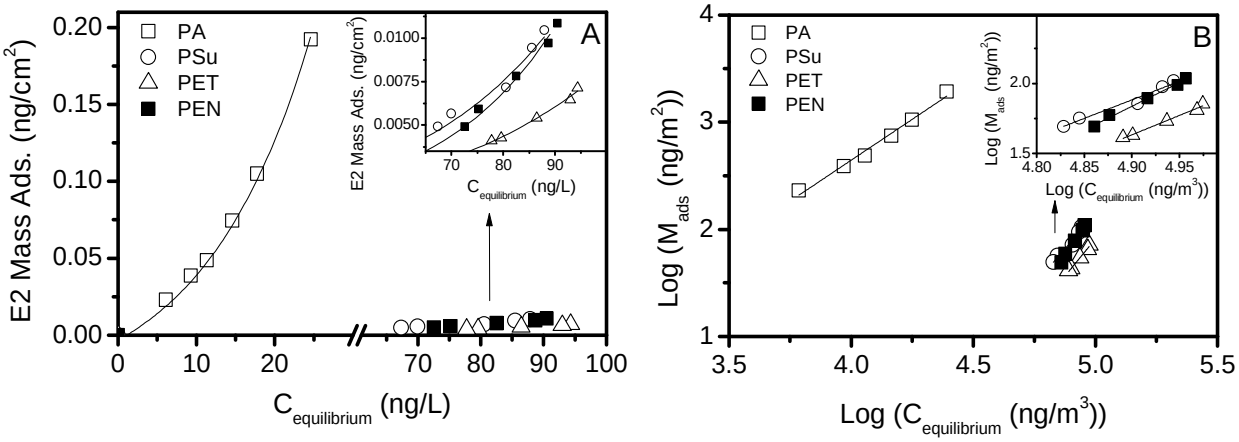

Figure 2 Estradiol (E2) static adsorption (A) isotherm onto different polymers (PA, PSu, PET and PEN, C_{feed}=100 ng.L^{-1}, 200 rpm, 25ºC) and (B) linear regression of the logarithmic form of the Freundlich isotherm. Triplicates of selected experiments were carried out and it was found that the E2 mass adsorbed varied by ±0.0005 ng/cm^2 and feed equilibrium concentration by ±0.12 ng/L

The correlation coefficient R^2 and the Freundlich isotherm coefficients are shown in Table 3. The slope $1/n_i$ obtained from Figure 2 B dictates the type of free energy involved in the sorption. Since $1/n_i>1$ for all the polymers (Table 3), this means that more sorbate (*i.e.* hormone) present in the sorbent (*i.e.* polymeric material) will enhance the free-energy of further sorption [31]. The sorbed molecules lead to a modification of the sorbent surface properties, enhancing further sorption [31]. The isotherm previously obtained in filtration mode for the NF270 membrane [5] was a Freundlich isotherm with n=1, *i.e.* a linear isotherm. In that case the shear stress caused by the cross-flow velocity might have prevented multilayer adsorption.

The polymer beads were assumed not to have internal porosity as according to the SEM pictures (not shown) there was no evidence of porosity. Furthermore, according to the manufacturer the beads absorb less than 3% water. This shows that very little volume of water can diffuse inside the polymer beads. Even less hormone would be able to diffuse inside the polymer as they have a

higher molecular weight (300 $g.mol^{-1}$) compared to water (18 $g.mol^{-1}$) so internal adsorption can be neglected. Finally, more than 60% of the hormone mass adsorbed onto the 4 polymers occurred in the first hour of the experiment and more than 80% occurred in the first 5 hours, showing that the adsorption occurs on the surface. If the polymers had fine pores and internal adsorption occurred, this process would be very slow as it would be diffusion dominated. Such is the case of the adsorption of nitrosamines in NF membranes [14].

The coefficient K_f can give an indication of the affinity of the hormone with the polymer. A higher K_f equates to a greater hormone adsorption capacity. The highest K_f was obtained for PA, followed by much smaller values for PSu and PE based polymers. This confirms the higher affinity of the hormones with PA compared to the other polymers. As can be seen in Figure 2 A, PA adsorbs higher amounts compared to any of the other polymers. PA adsorbs more than double at the lowest E2 concentration compared to the other polymers at the highest E2 concentration.

Table 3 Freundlich Isotherm Coefficients

Polymers	**R^2**	**$1/n_i$**	**K_f**
PA	0.99	1.5	$3.5.10^{-4}$
PSu	0.97	2.7	$7.6.10^{-12}$
PET	0.99	2.8	$1.0.10^{-12}$
PEN	0.99	3.4	$1.8.10^{-15}$

The significant difference in adsorption between the hormone and the different materials is yet to be explained. Hydrophobic interactions for example, do not explain this difference in interaction of the hydrophobic E2 (Log K_{ow}=4.01) [5] with PA compared to the other polymers. In fact, PA is the least hydrophobic polymer (*i.e.* lowest contact angle) and PSu the most hydrophobic (Table 2), despite PA adsorbing much higher amounts of E2. Hydrophobicity therefore does not explain adsorption of hormones onto these polymers [6]. Since hydrophobic interactions do not give a satisfactory answer, other types of interactions need to be considered, such as hydrogen bonding, dipole-dipole and π-π interactions [6].

Concerning the H-bond and π-π interactions, the hormones estrone E1 and estradiol E2 have several functional groups that can interact with several functional groups of the polymers:

- The benzene ring in the E1 and E2 phenol group is electron rich by resonance, caused by delocalization of electrons within the benzene molecule (Figure 3 A) allowing, in principle, for π- π stacking with an electron poor benzene ring of another molecule [32].
- The hydroxyl groups in the E1 and E2 and the ketone group in E1 can be strong H-bond donor and/or receiver (Figure 3 A and B). In fact, due to the previously mentioned

resonance stabilisation in the phenol, the H in this group is more acidic ($pK_a \approx 10$) and therefore more available for H-bonding than a regular hydroxyl group ($pK_a > 15$) [33].

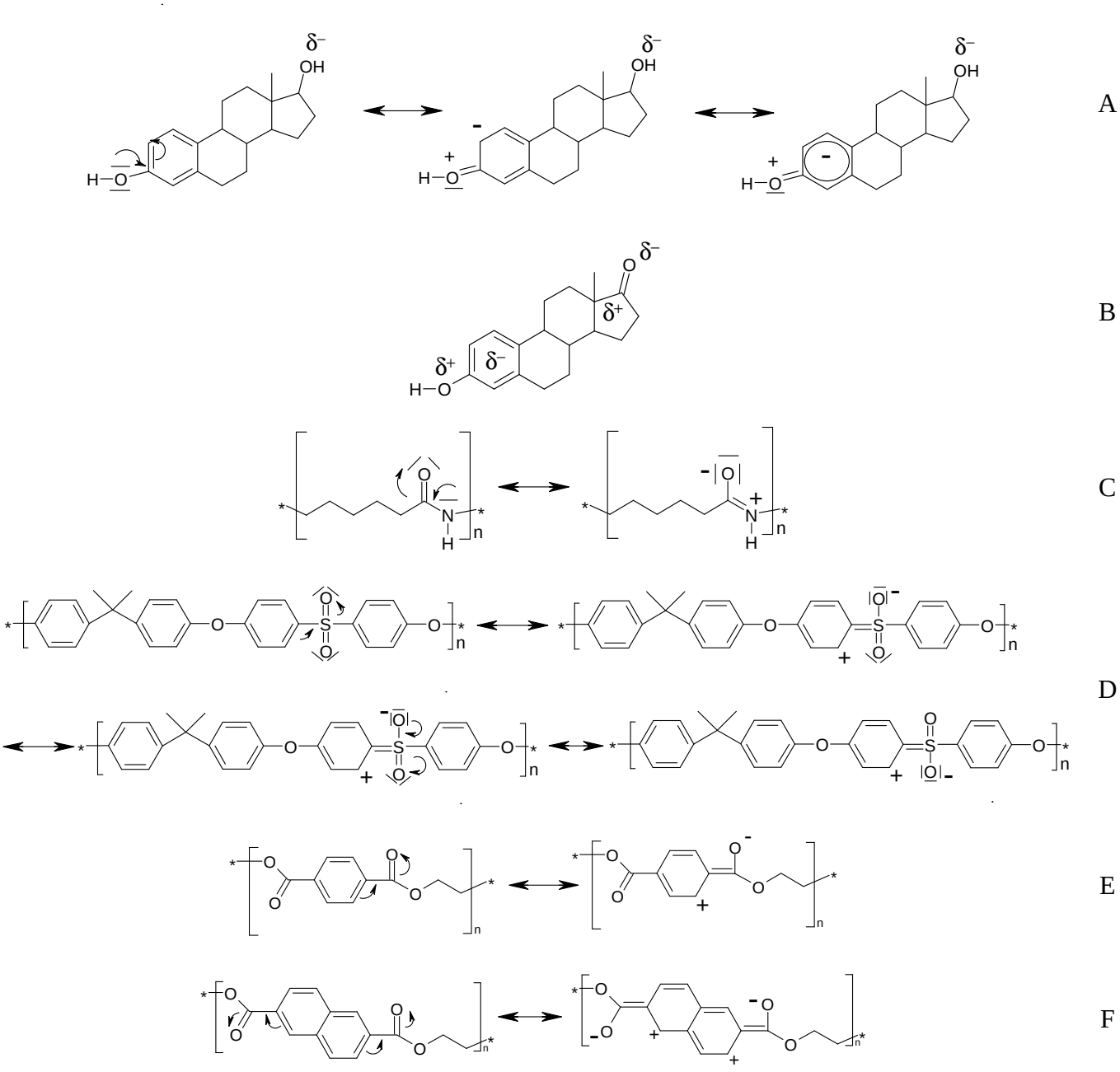

Figure 3 Electron density and resonance structures of A) estradiol (E2) and B) estrone (E1), A) polyamide (PA), B) polysulfone (PSu), C) polyethylene teraphthalate (PET) and D) polyethylene naphthalate (PEN) [33]

The polymers have functional groups that play a role in the interaction with the hormones:

- the resonance structure of PA shown in Figure 3 C originates a very polarised molecule, with a positively charged amine and negatively charged oxygen [33] which can form H-bonds with other molecules.

- The polymers PSu, PET and PEN on the other hand have a resonance structure shown in Figure 3 D, E and F. However these later resonance structures are known to result in poorly polarised benzene, sulphone and carboxyl groups [33] and hence the occurrence of H-bond and π- π stacking will most probably be weak. π - π stacking requires an electron-rich donor and an electron deficient receptor [34]. In consequence, these would form very weak interactions with the hormones compared to the H-bonding between the hormones and PA.

Compared to PA, PSu, PET and PEN have a lower capacity to form H-bonding which might explain the higher quantities of hormones adsorbed onto PA. Other types of interactions such as dipole-dipole and dielectric effects might be at play. However it is to date impossible to distinguish the contribution of each of these mechanisms individually.

TFC NF membranes are however not made of pure polymers and have a different degree of cross-linking. Surface modifications which are propriety of the manufacturer have been reported [21] and these modifications might have an impact on sorption. For example, the NF90 and BW30 membrane have the secondary amide groups characteristic of pure polyamide, whilst the NF270 with a higher degree of cross-linking, has tertiary amide groups. To confirm the adsorption isotherm results obtained with the different polymers, adsorption experiments in a diffusion cell were carried out with the NF 270 membrane, as described in the next section.

3.2. Adsorption onto TFC NF membranes

TFC NF membranes are made of three different layered materials (PA_m, PSu_m and PE_m) which are physically impossible to separate from each other. It is however possible to confirm if the hormones preferentially adsorb onto the active layer by physically peeling the PA_m+ PSu_m layers from the PE_m layer of the NF 270 membrane and placing PA_m+PSu_m in a diffusion cell, each side facing a separate cell. This allows exposing the PA_m and PSu_m layers to a determined concentration on each side independently. Results are presented in Figure 4 for an exposed time of 8 hours.

Despite possible surface chemistry modifications, PA_m is found to adsorb much higher amounts of E1 and E2 than the support PSu_m layer, confirming a higher affinity of the hormone with the polyamide active layer. When exposed to the same concentrations, PA_m adsorbs at least 2.5 times more than PSu_m for both hormones. For 100 $ng.L^{-1}$ of E1 and E2, PA_m adsorbed 4 ng and 3 ng, respectively, whilst PSu_m adsorbed 1.6 ng and 1 ng, respectively.

In reality, the active layer is in the first instances of filtration in contact with the concentration at the membrane surface (>100 $ng.L^{-1}$), compared to the PSu_m layer, subjected to a much lower concentration, *i.e.* the permeating concentration (20 $ng.L^{-1}$ for E1 and 30 $ng.L^{-1}$ for E2

[5]) due to hormone retention and sorption by the active layer. At these concentrations, PA_m adsorbs 14 and 10 times higher mass than PSu_m for E1 and E2, respectively. Whilst PA_m adsorbed 3.6 ng of E1 and 3 ng of E2 at 100 ng.L^{-1}, PSu_m adsorbed 0.23 ng of E1 at 20 ng.L^{-1} and 0.29 ng of E2 at 30 ng.L^{-1}.

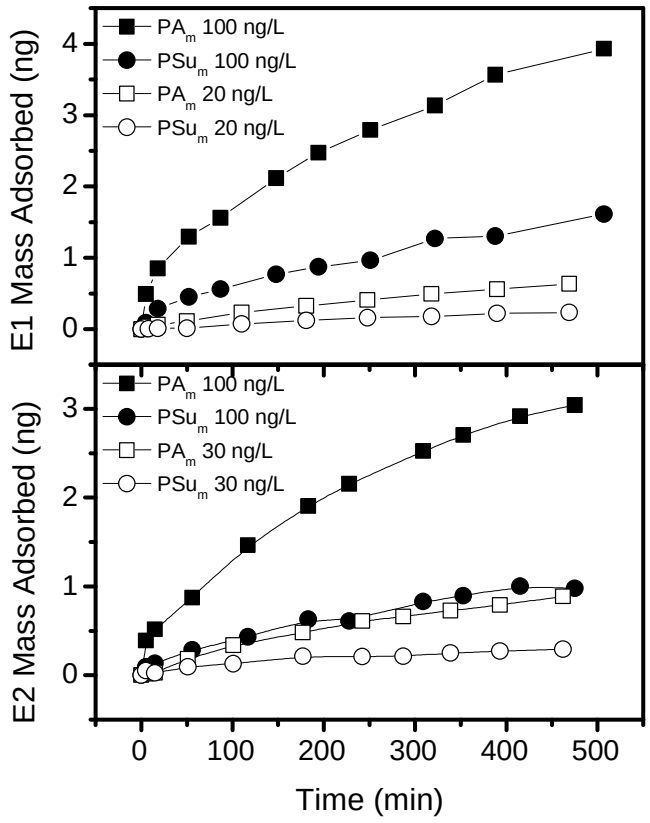

Figure 4 Estrone (E1) and estradiol (E2) adsorption onto the polyamide (PA) and polysulfone (PSu) sides of the NF270 membrane tested in a diffusion cell (pH 7, 1000 rpm, $C_{feed\ E1\text{-}PA}$= 100 ng.L^{-1}, $C_{feed\ E1\text{-}PSu}$=20 ng.L^{-1}, $C_{feed\ E2\text{-}PA}$=100 ng.L^{-1}, $C_{feed\ E2\text{-}PSu}$=30 ng.L^{-1}, PES support layer removed, 4.9 cm^2 of membrane area exposed, 125 mL of cell volume). Triplicates of selected experiments were carried out and it was found that the hormone mass adsorbed varied by ±0.076 ng for PA and ±0.066 ng for PSu

It is possible to compare the adsorption results obtained with the polymer experiments in Figure 2 and the diffusion cell experiments in Figure 4. Considering the equilibrium concentrations obtained in the diffusion cell for each layer after adsorption has occurred and using these equilibrium concentrations in the Freundlich isotherm obtained for each polymer allows the comparison of the mass adsorbed between the TFC layers and the raw polymers (Table 4).

Table 4 Comparison between E2 diffusion cell adsorption and the polymer Freundlich isotherm

Diffusion Cell Feed Conc. ($ng.L^{-1}$)	PA_m Conc.$_{equil}$ ($ng.L^{-1}$)	PA_m Mass adsorbed ($ng.cm^{-2}$)	PSu_m Conc.$_{equil}$ ($ng.L^{-1}$)	PSu_m Mass adsorbed ($ng.cm^{-2}$)
100	80	0.61	95	0.18
30	24	0.20	29	0.06

Freundlich isotherm Feed Conc. ($ng.L^{-1}$)	PA_m Conc.$_{equil}$ ($ng.L^{-1}$)	PA Mass adsorbed ($ng.cm^{-2}$)	PSu_m Conc.$_{equil}$ ($ng.L^{-1}$)	PSu Mass adsorbed ($ng.cm^{-2}$)
100	80	0.79	95	0.02
30	24	0.13	29	0.001

Comparing the amount adsorbed onto the different layers considering adsorption occurs only on the surface of the TFC layer gives very similar results between the PA_m layer and the PA polymer. This is expected as the PA_m layer is very dense and penetration and diffusion of the hormone will be very slow. In the study by Nghiem [35] it took more than 8 hours to detect hormone on the permeate side of the NF270 membrane in a diffusion cell, with the active layer exposed to 100 $ng.L^{-1}$ and the support layers exposed to pure water. In our study however, both cells started with the same E2 concentration (*i.e.* 100 $ng.L^{-1}$) so the driving force for transport, in this case concentration, is lower compared with the one in Nghiem's study. One can therefore assume that most of the PA_m adsorption occurred on the surface.

For the PSu_m layer and the PSu polymer the mass adsorption results are an order of magnitude higher in the diffusion cell. It has to be noted however that an accurate determination of the mass adsorbed per surface area is not possible in the diffusion cell experiments as the PSu_m layer is of the UF type and therefore diffusion of the hormone inside the PSu_m layer occurs. In fact, as stated in section 2.5, after 8 hours water penetrates the PSu_m layer and appears on the PA_m layer cell, showing that the solution is in contact with the internal surface area of the PSu_m layer.

Thus, the isotherms obtained with the polymeric materials can be used to compare the mass adsorbed of the hormone onto the different TFC layers, showing that the hormone has a much higher affinity for the PA_m layer compared to the PSu_m layer. Most of the adsorption will therefore occur on the PA_m active layer.

It can be argued that the amount adsorbed onto the PSu_m layer during filtration experiments will be much higher than the one adsorbing onto the PA_m layer as the first one is thicker than the later one. According to the study by Pacheco *et al.* [36], the support PSu_m layer has a thickness of 30 µm. Assuming a porosity of 0.06 [37], an average pore radius of 50 nm [37, 38] for the PSu_m layer and the width and length of the cross-flow membrane cell used in this study, an

internal surface area of 0.331 m^2 for the PSu_m support layer using equation (3) is obtained. The hormone permeate concentration in contact with the PSu_m layer are an average of 20 $ng.L^{-1}$ [5].

Considering a PA nanofiltration total area for the NF270 membrane of 0.0134 m^2 (as discussed in the next section – see Table 6), a hormone concentration inside the membrane pore of 6.5 $ng.L^{-1}$ (due to partitioning on the NF membrane), a concentration of 140 $ng.L^{-1}$ on the membrane surface [5] and the Freundlich isotherms obtained in Table 3, the amount adsorbed on the PSu_m layer is less than 2% of the total mass adsorbed on the membrane. For membranes with thicker active layer, this difference will be higher. This difference in mass adsorbed obtained shows that the PA_m layer adsorbs most of the hormones compared to the support PSu_m layer.

Now that it has been established that the bulk of the adsorption occurs on the active layer, the next step is to study the influence of the active layer characteristics, such as pore radius and internal surface area in the retention and adsorption of hormones.

3.3. Pore Size and Surface Area Effect on Retention and Adsorption

To determine pore radius and internal surface area effect in the adsorption and retention of hormones, five NF membranes were characterised for average pore radius (r_p) and active layer thickness to porosity ratio (δ/ε) [39, 40]. This is possible by applying the hydrodynamic model [41] which only considers steric interactions between the membrane and inert tracer organic solutes (*i.e.* non-adsorbing and non-charged solutes). The membrane pores are assumed as cylindrical capillary tubes with an average pore radius r_p and length δ. The characterisation method adopted is described in Nghiem *et al.* [17]. The organic tracers used in the characterisation are presented in Table 5, along with their diffusivities (D_∞) and equivalent solute radius (r_s). D_∞ were either obtained from the literature (Table 5) or were calculated with the Wilke and Chang equation [42] for dioxane or the Worch equation [43] for the case of methanol. The solute radius r_s was determined with the Stokes-Einstein equation [41].

Table 5 Organics Characteristics

Organics	**MW ($g.mol^{-1}$)**	**D_∞ ($m^2.s^{-1}$)**	**r_s (nm)**
methanol	32	1.5×10^{-9} [43]	0.13
dioxane	88.11	9.82×10^{-10} [42]	0.24
xylose	150.13	7.50×10^{-10} [44]	0.31
dextrose	180.16	6.80×10^{-10} [45]	0.34

The value of r_p and δ/ε are obtained using an optimization method (Solver Microsoft Excel) by fitting the theoretical real retention, given by equation (1) to the experimental real retention given by equation (2).

$$R_r = 1 - \frac{\Phi K_c}{1 - \exp(-Pe)(1 - \Phi K_c)} \quad (1)$$

where Pe is the Peclet number ($Pe = \frac{K_c J_v}{K_d D_\infty} \frac{\delta}{\varepsilon}$), Φ is the partition coefficient given by $\Phi=(1-\lambda)^2$, with $\lambda=r_s/r_p$, r_s (m) is the equivalent solute radius and r_p (m) is the membrane average pore radius. The coefficients K_c and K_d, which depend only on λ, are the diffusion and convective hindrance factors calculated using the Bungay and Brenner coefficients reviewed by Deen [41]. J_v is the permeate flux ($m.s^{-1}$) and D_∞ ($m^2.s^{-1}$) are the organics diffusion coefficient in the liquid medium.

The experimental real retention R_r in equation (2) was calculated with the results of the observed retention R_0 as a function of pressure, or permeate flux J_v, for the organics in Table 5.

$$\ln\frac{1-R_r}{R_r} = \ln\frac{1-R_0}{R_0} - \frac{J_v}{k_f} \quad (2)$$

where k_f ($m.s^{-1}$) is the mass transfer coefficient determined with the Sutkover method with 0.1 M NaCl at Q_{feed}=2 $L.min^{-1}$ (to avoid polarisation) and two different pressures (7 and 11 bar) [46]. The mass transfer coefficient for each organic was corrected in relation to the NaCl one [47]. For the TFC-SR2, the Sutkover method is not applicable due to an increase in permeate flux when salt is present compared to the pure water flux at the same pressure. The Deissler Sherwood [48] correlation in cases of minimised polarisation was therefore applied in this case.

Results for the theoretical real retention (equation 1) fitted to the experimental retention (equation 2) are shown in Figure 5 for the NF270 and TFC-SR2 1 membranes. The NF 270 membrane shows higher retentions for all the organic compounds, which is expected given the smaller pore radius. In the study by Verliefde *et al.* [4] it was shown that compounds that interact with the nanofiltration membrane should have a steric partition coefficient modified with a solute-membrane affinity coefficient. However, in our study this coefficient was assumed to be negligible for the trace organics and membranes used as the results obtained for the r_p and δ/ε were consistent for each membrane characterised (Table 6).

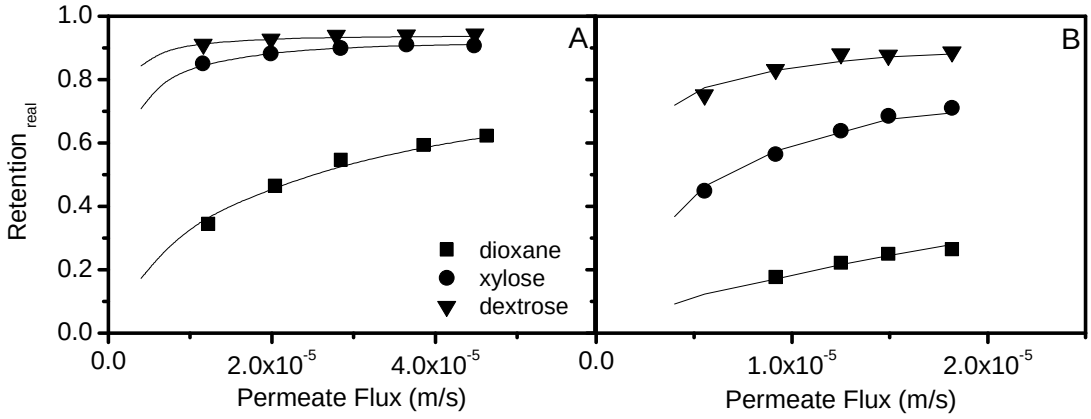

Figure 5 Real retention as a function of permeate water flux for the different organic tracers for the A) NF 270 and B) TFC-SR2 1 (Cross-flow conditions: C_{feed}=25 mgC.L^{-1}, Re_h= 1450, pH 7, 24°C)

Once the parameters r_p and δ/ε are obtained, the porosity ε can be calculated using estimate values of the active layer thickness δ for each membrane (Table 1). With ε, the total area available for adsorption is estimated considering the internal surface of pores as perfect cylinders of length δ and average pore radius r_p. After algebraic manipulation the total effective interfacial area of the active layer (*i.e.* membrane surface and internal area) is obtained with equation (3):

$$A_{total} = A_{sm} + A_p = WL(1-\varepsilon) + \frac{2WL\varepsilon\delta}{r_p} \qquad (3)$$

where W (m) and L (m) are the membrane width and length, respectively, A_{total} (m^2) is the total effective interfacial surface area available for adsorption, A_{sm} (m^2) and A_p (m^2) are the estimated membrane surface and internal pore surface area, respectively. Results obtained for the several membranes are presented in Table 6. Results for average pore size and thickness to porosity ratio are consistent with the literature [39, 49]. The variability in A_{total} (Table 6) was calculated in equation (3) using the error propagation method considering the variability in porosity ε, pore radius r_p and membrane thickness δ (refer to Support Information B).

In reality the NF membranes will have a pore size distribution [50]. An average pore size is however used by many researchers in order to simplify the model used for membrane characterisation or transport of organic solutes [4, 17, 39, 40, 49, 51].

The effective interfacial area of the active layer (surface area and internal pore area) is dependent on the active layer pore radius, porosity and active layer thickness (equation 3). It increases with membrane thickness and porosity increase for a constant pore size and decreases with pore radius increase for a constant porosity. The NF 270 membrane has the smallest effective

interfacial area because of a small thickness and large pore radius. In contrast, the TFC-SR2 1 has one of the highest effective interfacial areas despite having slightly bigger pores than the NF 270. This is because it has a very thick active layer.

In this work the tortuosity of the pores and the surface roughness were not considered in the calculation of the surface and internal area available for sorption. Tortuosity has not been determined for NF membranes due to the lack of analytical tools.

Table 6 Membrane pore radius (rp) and thickness/porosity (δ/ε) ratio determination. The membrane active layer thickness is given in Table 1

Membranes	**Average Pore Radius r_p (nm)**	**Active Layer Thickness Porosity Ratio δ/ε (μm)**	**Effective Interfacial Area of Active Layer A_{total} (cm^2)**	**Porosity**
BW30	0.32 ± 0.01	5.38 ± 1.48	2953 ± 1776	0.04 ± 0.02
NF90	0.34 ± 0.04	0.83 ± 0.21	15439 ± 6700	0.26 ± 0.08
TFC-SR2 2	0.52 ± 0.03	2.45 ± 0.08	8501 ± 1497	0.14 ± 0.01
TFC-SR2 1	0.46 ± 0.01	1.09 ± 0.06	21461 ± 3191	0.32 ± 0.03
TFC-SR3	0.38 ± 0.01	1.60 ± 0.04	23817 ± 1728	0.25 ± 0.01
NF 270	0.42 ± 0.02	1.10 ± 0.04	134 ± 18	0.020 ± 0.002

It is possible to compare the experimental permeability obtained with the one calculated from the Hagen-Poiseuille equation [52] with the values obtained for pore radius r_p and thickness to porosity ratio δ/ε. The results obtained for each membrane are presented in Table 7.

Table 7 Comparison between the experimental and Hagen-Poiseullie permeabilities

Membrane	**Experimental Permeability (m/s)**	**H-P permeability (m/s)**
BW30	1.25×10^{-5}	2.81×10^{-6}
NF90	3.24×10^{-5}	2.05×10^{-5}
TFC-SR2 2	3.82×10^{-5}	1.63×10^{-5}
TFC-SR2 1	2.20×10^{-5}	2.86×10^{-5}
TFC-SR3	2.05×10^{-5}	1.33×10^{-5}
NF270	5.19×10^{-5}	2.36×10^{-5}

As can be seen from Table 7, the permeabilities obtained with the Hagen-Poiseuille equation are similar to the experimental ones. Deviations however, will occur as the Hagen-Poiseuille equation assumes that the fluid is viscous inside the membrane and that the pores have a constant cross-section. Considering the sizes of pores in NF, these two assumptions are debatable,

as for example, no tortuosity is taken into account. This will be especially pronounced for the BW30 membrane which is thick and denser than the other membranes.

In regards to the surface roughness, there is no available direct relationship between this and the membrane surface area. AFM has however been used to estimate the surface area of membranes taking the roughness into account. It was estimated that a projection area of 100 μm^2 gave areas between 150 and 180 μm^2 for an average surface roughness between 40 and 85 nm [53]. For the roughest membranes used in this study, the BW 30 and the NF 90, the internal pore area estimated is at least 70 times higher than the surface area. In that case, the increase of surface area caused by the membrane roughness has a very small impact in the effective interfacial area of the active layer. Considering double the surface area caused by a roughness of 60 nm (Table 1), the total membrane area estimated would be of 2996 cm^2 for BW30 and 15472 cm^2 for the NF 90 membrane instead of 2953 cm^2 and 15439 cm^2 (Table 6), respectively. The other membranes used have a very low roughness which will have a minimal impact on the membrane effective interfacial area.

The effect of pore radius in the adsorption and retention of E2 is shown in Figure 6. An increase in pore radius r_p from 0.32 nm to 0.52 nm leads to a decrease in the steric exclusion capacity of the membrane and a higher partitioning of the hormones inside the membrane pores, according to the hydrodynamic model [41]. This leads to an increase in adsorption from 0.17 $ng.cm^{-2}$ to 1.10 $ng.cm^{-2}$ and a decrease in retention from 88% down to 34% (Figure 6 A and B at pH 7). This trend is especially pronounced for membranes with r_p>0.42 nm seeing the estimated hormone radius is r_{E2}=0.4 nm [54]. A similar trend was obtained by Nghiem *et al.* [12] where an RO membrane adsorbed less than NF membranes. The fact that the retention of the hormone decreases with increase of membrane pore size shows that despite the existence of a pore size distribution, the usage of an average pore radius is still representative of the membrane performance.

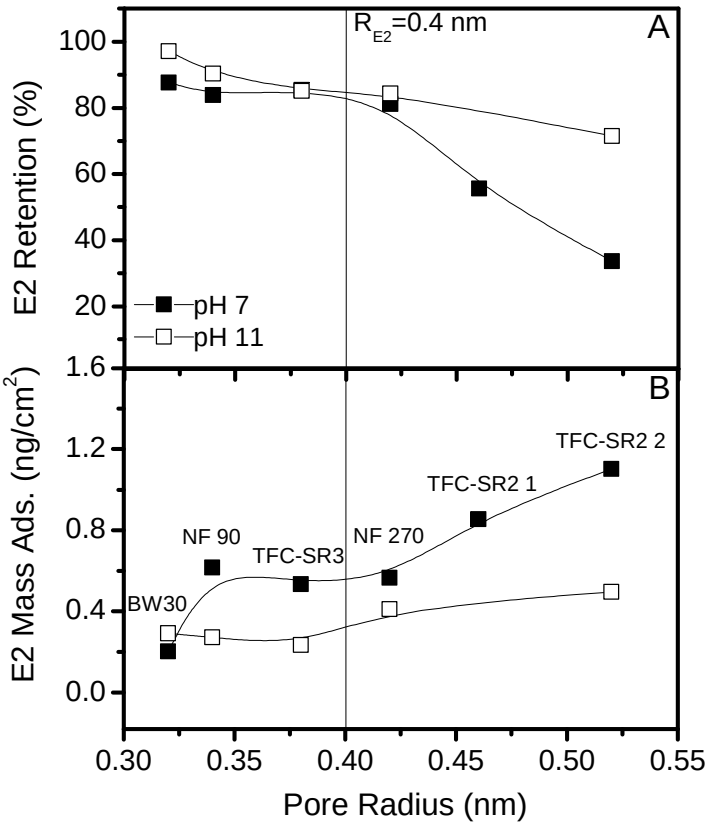

Figure 6 Estradiol (E2) retention and mass adsorbed (Mass Ads.) per cross-flow cell surface area (ng.cm^{-2}) with increasing effective average pore radius; membranes used are presented in Table 6 (Cross-flow conditions: $C_{feed\ initial}$=100 ng.L^{-1}, 24°C, 11 bar, Re_h=1450, and pH 7 and 11). Triplicates of selected experiments were carried out and it was found that steady-state retention did not vary by more than ± 5%, total mass adsorbed by ± 0.08 ng.cm^{-2} and J/J_0 by ± 0.02

For the membrane with a pore radius r_p=0.34 nm (NF 90), the mass adsorbed per area of the cross-flow cell is about four times higher, 0.64 ng.cm^{-2}, compared to the membrane with a similar pore radius r_p=0.32 nm (BW 30), 0.17 ng.cm^{-2}. It could be argued that membranes with higher permeability (Table 1) and therefore a higher concentration polarisation such as the NF90 compared with the BW30, would adsorb higher mass of hormones [5]. However, when comparing membranes with similar permeabilities such as the TFC-SR2 2, the TFC-SR3 and the BW30 and the membranes NF 90 and TFC-SR2 1 (Table 1), the trend shows an increase with pore radius (Figure 6 B) rather than membrane permeability. Furthermore, the experiments were carried out at conditions of minimised polarisation (Re_h=1450 or Q_{feed}=2 L.min^{-1} [5]).

Besides the pore radius effect on adsorption and retention, other effects might be at play which might affect adsorption onto NF membranes: hormone-membrane affinity and internal surface area. As previously mentioned, the difference that surface roughness causes in the effective interfacial area is minimal.

As previously mentioned, the TFC membranes are modified with additives on the active layer, which is likely to affect hormone affinity. By analysing the static isotherms obtained for E2 with the NF 90 and the BW 30 membranes, one can see that the hormone affinity for these two membranes is very similar (Figure 7), thus not explaining the higher adsorption obtained for the NF 90 membrane.

The hormone isotherm with the two batches of the TFC-SR2 membranes (1 and 2) is very similar to the ones obtained for the NF 90 and BW 30 (Figure 7). The difference in mass adsorption obtained in Figure 6 is therefore caused by a pore size effect.

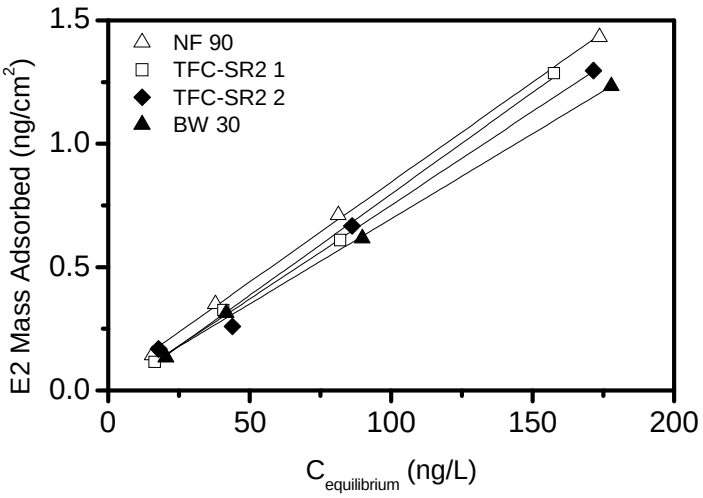

Figure 7 Estradiol (E2) static isotherm (no pressure) for the NF 90, the BW 30 and the TFC-SR2 1 and 2 membranes ($C_{feed\ initial}$=24, 50, 100 and 200 ng.L^{-1}, 24°C, 200 rpm and pH 7)

If the effective interfacial area of the active layer is taken into account (Table 6), in general an increase of the total effective interfacial surface area increases the hormone mass adsorbed per cross-flow surface area, showing that internal surface area plays a role in adsorption (Figure 8):

- The BW30 and the NF 90 membranes have similar pore radius (0.32 and 0.34 nm, respectively), but since the NF 90 has a higher surface area of 15439 cm^2 compared to 2953 cm^2 for the BW 30 (Table 6), it adsorbs more E2.
- The NF 270, NF 90 and TFC-SR3 adsorb similar E2 mass per cross-flow surface area (around 0.55 ng.cm^{-2}) despite the NF 270 membrane having a bigger pore radius 0.42 nm compared to 0.34 nm for the NF 90 and 0.38 nm for the TFC-SR3. These later two have a much higher internal surface area (15439 cm^2 for the NF 90 and 23817 cm^2 for the TFC-SR3) compared to the NF 270 membrane (134 cm^2) compensating for a smaller pore radius.

- The TFC-SR2 1 and 2 have higher surface area and pore radius than the NF 270 membrane (Table 6) and therefore adsorb more mass per cross-flow surface area (Figure 8).

Hormone filtration by NF membranes at neutral pH indicates penetration and internal pore sorption. However, at alkaline pH, when the hormone is dissociated the occurrence of electrostatic repulsion might interfere in the hormone adsorption mechanism.

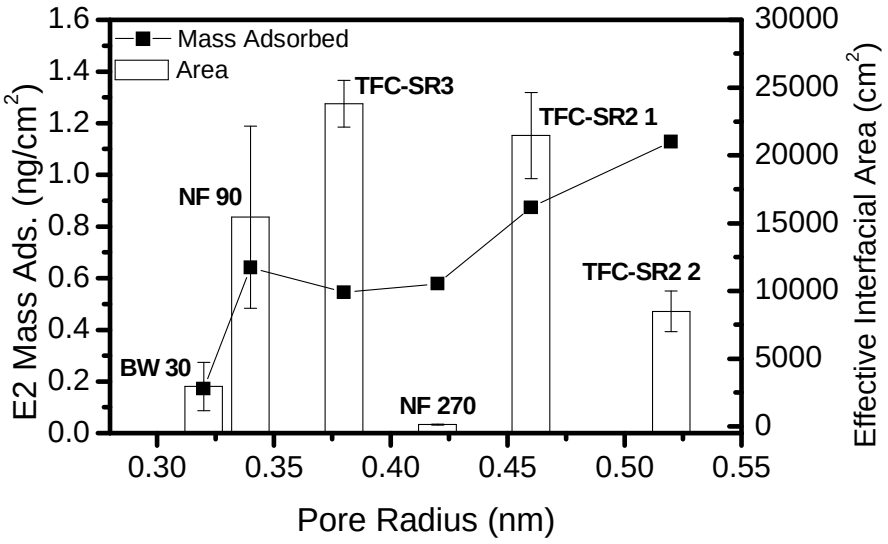

Figure 8 Estradiol (E2) mass adsorbed per cross-flow surface area (Mass Ads.) ($ng.cm^{-2}$) and membrane effective interfacial area A_{total} (cm^2) with increasing effective pore radius (Table 6) (Cross-flow conditions: $C_{feed\ initial}$=100 $ng.L^{-1}$, 24°C, 11 bar, Re_h=1450, pH 7). The variability in A_{total} is presented as error bar.

At pH 11 hormone adsorption per cross-flow surface area increases with pore radius from 0.27 $ng.cm^{-2}$ to 0.50 $ng.cm^{-2}$, and the retention decreases from 97% to 71% (Figure 6). However, due to electrostatic repulsion between the negatively charged membrane (Table 1) and the dissociated hormone ($pK_{a\ E1,E2}$ = 10.4), the mass adsorbed per cross-flow surface area is lower and the retention is higher compared to pH 7 [15, 19]. Although the hormone phenol group is negatively charged at pH 11 (Figure 3 A and B) and electrostatic repulsion by the membrane occurs, the hormone is still able to form hydrogen bonding with the membrane through the ketone group of E1 and the hydroxyl group of E2. At pH 11 the effect of pore radius is not very pronounced compared to pH 7, indicating that adsorption occurs on the surface, whilst at pH 7 partitioning and penetration inside the active is more predominant. This can be explained with electrostatic repulsion reduced penetration.

In Figure 9 adsorption kinetics is represented for a tight (NF90, r_p=0.34 nm) and a loose (TFC-SR2 2, r_p=0.52 nm) membrane at pH 7 and 11. At pH 7 the mass adsorbed per cross-flow surface area increases gradually with time until it reaches steady-state and saturation is reached more quickly for the loosest membrane: it takes 100 minutes for the looser membrane to reach 80% of the total mass adsorbed compared to 200 minutes for the tighter membrane. A slower penetration inside the membrane pores and consequent slower adsorption is likely to occur on the tighter membrane, indicating internal adsorption.

At pH 11 the mass adsorbed per cross-flow surface area increases sharply in the first 5 minutes and quickly reaches steady-state: adsorption occurs mainly at the membrane surface with some penetration occurring for the loosest membrane due to the difference between the hormone radius (0.4 nm) and the pore radius (0.52 nm). Steinle-Darling *et al.* [18] found that charged trace contaminants reached adsorption saturation quickly while uncharged ones took several days to reach saturation.

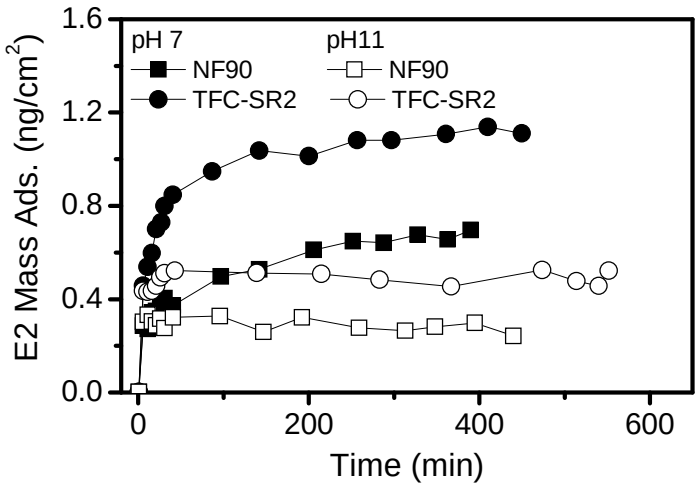

Figure 9 Estradiol (E2) mass adsorbed per cross-flow surface area (Mass Ads.) for the NF90 and the TFC-SR2 2 membrane for pH 7 and 11. (Cross-flow conditions: $C_{feed\ initial}$=100 ng.L^{-1}, Re_h=1450, 11 bar, 24°C)

E1 desorption from membranes saturated in static and filtration mode at different pressures confirms internal adsorption. Figure 10 shows the percentage of E1 mass extracted for several pressures in relation to the total mass adsorbed.

Extraction efficiency decreases with increase of pressure (Figure 10). The percentage of E1 static extraction from pressure experiments decreases from 100% for 1 bar (*i.e.* no pressure applied) to <20% for 15 bar. Kimura *et al.* [20] obtained lower extraction of trace contaminants from pressure experiments (40%-60% recovery) when compared to static experiments (around 100%

recovery). An increase of pressure increases the concentration at the membrane surface. In this case, more hormone partitions into the membrane active layer pores, causing a higher adsorption inside the active layer [5]. Since internal access for extraction in static mode is difficult, the extraction efficiency decreases with increase of pressure. In consequence a desorption efficiency is an indicator for hormone penetration.

When filtered extraction is carried out with MilliQ water at 11 bar, a much higher extraction is obtained (82%) [15] compared to the static extraction (no pressure, 25%). Filtered MilliQ water has access to hormones adsorbed internally. Subsequent filtration with 2% acetone recovered a further 7% of E1, showing internal adsorption on the active layer.

The PE layer that had been separated from the other two layers, consistently desorbed less than 2% of the total hormone mass adsorbed, showing a low adsorption onto the PE layer, confirming previous results of polymer adsorption.

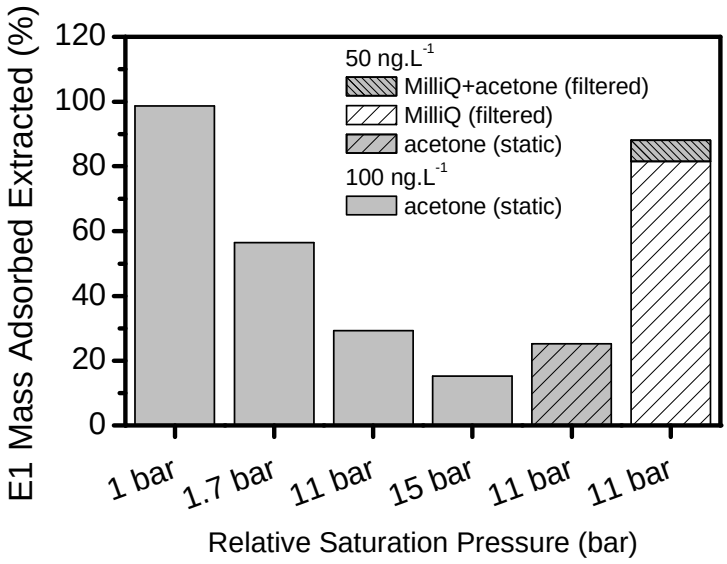

Figure 10 Estrone (E1) mass adsorbed extracted (%) from the NF270 membrane for different pressures used to saturate the membranes (filtered extraction in cross-flow: T=24ºC, Re_h=427, P=11 bar, MilliQ water, then MilliQ+acetone solution (2%); static extraction: T=24ºC, 200 rpm, acetone). Triplicates of selected experiments were carried out and it was found that the variability in hormone extraction was of ± 8.5% for filtration experiments

Pore size and internal surface area have been shown to be important parameters in the transport of adsorbing compounds through the active layer when the hormone is not dissociated. Pore size, or steric exclusion plays a role in adsorption since it allows or prevents access to the internal surface area. The internal surface area will then determine how much adsorption occurs

internally. These two membrane characteristics are important in modelling hormone adsorption on NF membranes.

To better understand the effect of pore radius and internal surface area, a simple conceptual schematic is shown in Figure 11. For a membrane of same pore radius r_{p1} but increased active layer thickness ($\delta_1 > \delta_2$), a higher internal area is available, increasing the total hormone adsorption. For a membrane with the same active layer thickness δ_2 but increased pore radius $r_{p2} > r_{p1}$ more hormone partitions into the pore, according to the hydrodynamic model [41]. The concentration inside the membrane pore will therefore be higher, increasing the adsorption per area. This is a very simplistic approach because in reality the membranes have different pore radius and active layer thicknesses. Thus a combination of the effect of pore radius, or partitioning, and internal surface area, or membrane thickness, will impact on the concentration profile inside the membrane pores and hence will impact on adsorption. To clearly establish the different effects in hormone adsorption onto NF membranes caused by different pore sizes and membrane thicknesses, a new transport model taking these factors into account needs to be developed.

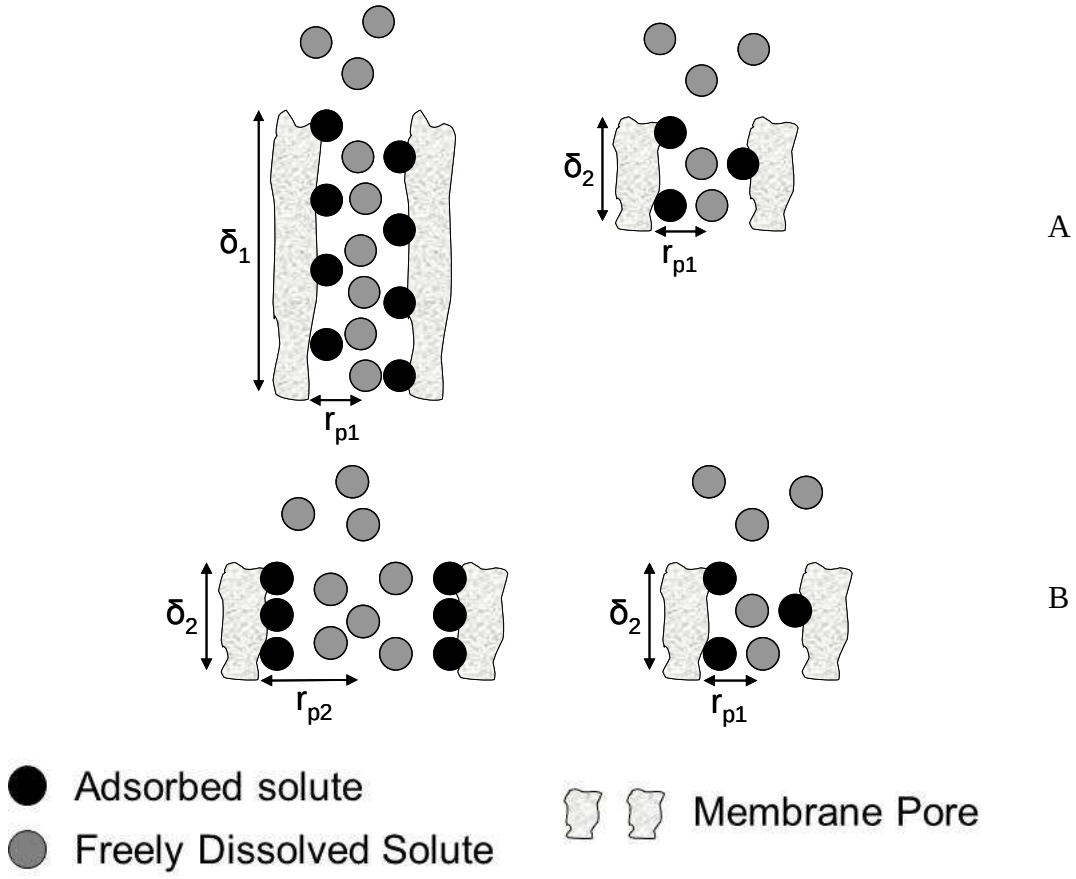

Figure 11 Conceptual schematic of the effect of (A) internal surface area (*i.e.* active layer thickness δ) and (B) pore radius r_p (*i.e.* partitioning) in hormone adsorption in the active layer

4 Conclusions

Several membrane parameters are required to describe adsorption and retention of hormones onto NF membranes. Polyamide and the PA active layer of TFC NF membranes were found to adsorb much higher quantities of hormone than any of the other materials of the membranes showing that, for hormones, the bulk of the adsorption occurs in the active layer. As concluded in the study of Ben-David *et al.* [55], the usage of polyamide NF membranes in water treatment poses a problem in the removal of trace contaminants due to the interaction of these with the active layer. From the results presented here, hormones which have a high endocrine potency are included in this family of contaminants. Other materials should therefore be considered in the making of NF and RO membranes, justifying future work focusing on the interaction between trace contaminants and different polymeric materials.

The active layer pore radius was found to be a determining factor in the removal of adsorbing contaminants in NF membranes. Steric exclusion determines the amount of hormone that penetrates (*i.e.* partitions) inside the pore and therefore controls access to the internal surface area.

On the other hand, the hormones were shown to adsorb internally at pH 7, in contrast to surface adsorption at pH 11 due to electrostatic repulsion. The active layer internal area available contributes alongside with the pore radius to the amount of hormone that can be adsorbed internally. This suggests that if trace contaminant adsorption is to be avoided, trace contaminant partitioning inside the active layer should be minimised, as well as the internal surface area.

Acknowledgements

We would like to thank the University of Edinburgh for the studentship and project funding provided to Andrea Semiao, Dow Filmtech and Koch membranes for providing the membrane samples, Dr. Nuno Maulide (Max-Planck-Institut für Kohlenforschung, Germany), for his discussions on polymer adsorption, Helfrid Rossiter and Dr. Chris Jeffree (University of Edinburgh) for the TFC-SR2 2 TEM images, Ime Akanyeti for her collaboration in grinding the polymers, Annalisa De Munari, Dr. Alexander Bismarck and Dr. Kingsley Ho (Imperial College, UK) for the zeta potential measurements and Laura Richards and Helfrid Rossiter for the NF 90 and TFC SR2 1 membrane characterisation.

A very special thank you is given to Prof. Polizzi (Universita Ca’ Foscari Venezia, Italy) for his TEM measurements of several membranes for the determination of the active layer thickness and variability of the NF 90, NF 270 and TFC-SR 2 1 membranes.

Supporting Information

A_{total} variability calculation

The total membrane surface area available is calculated with equation (B1):

$$A_{total} = A_{sm} + A_p = WL(1-\varepsilon) + \frac{2WL\varepsilon\delta}{r_p} \quad \text{(B1)}$$

To determine the uncertainty of A_{total} caused by variability of its parameters such as ε, δ, and r_p, the error propagation method was applied (equation B2):

$$\Delta A_{total}^{\ 2} = \left|\frac{\partial Atotal}{\partial \varepsilon}\right|^2 \Delta\varepsilon^2 + \left|\frac{\partial Atotal}{\partial \delta}\right|^2 \Delta\delta^2 + \left|\frac{\partial Atotal}{\partial r_p}\right|^2 \Delta r_p^{\ 2} \quad \text{(B2)}$$

The uncertainty of A_{total} is given by:

$$\Delta A_{total}^{\ 2} = \left|-WL + \frac{2WL\delta}{r_p}\right|^2 \Delta\varepsilon^2 + \left|\frac{2WL\varepsilon}{r_p}\right|^2 \Delta\delta^2 + \left|\frac{-2WL\varepsilon\delta}{r_p^{\ 2}}\right|^2 \Delta r_p^{\ 2} \quad \text{(B3)}$$

The variability of each parameter Δδ and Δr_p is provided in Table 1 and Table 6, respectively. The variability of Δε was calculated from error propagation from equation (B4):

$$\varepsilon = \frac{\delta}{(\delta/\varepsilon)} = \frac{\delta}{A} \quad \text{(B4)}$$

Where δ is the membrane thickness (Table 1) and (δ/ε), or A, is the parameter thickness to porosity ratio obtained from fitting equation (1) to equation (2), as discussed in the paper. Its variability is provided in Table 6.

Propagation of equation (B4) gives equation (B5) and (B6):

$$\Delta\varepsilon^2 = \left|\frac{\partial\varepsilon}{\partial A}\right|^2 \Delta A^2 + \left|\frac{\partial\varepsilon}{\partial\delta}\right|^2 \Delta\delta^2 \quad \text{(B5)}$$

$$\Delta\varepsilon^2 = \left|-\frac{\delta}{A^2}\right|^2 \Delta A^2 + \left|\frac{1}{A}\right|^2 \Delta\delta^2 \qquad \text{(B6)}$$

References

[1] M. Rabiet, A. Togola, F. Brissaud, J.-L. Seidel, H. Budzinski, F. Elbaz-Poulichet, Consequences of treated water recycling as regards pharmaceuticals and drugs in surface and ground waters of a medium-sized mediterranean catchment, Environ. Sci. Technol., 40 (2006) 5282-5288.
[2] J.P. Sumpter, Endocrine disrupters in the aquatic environment: an overview, Acta Hydrochim. Hydrobiol., 33 (2005) 9-16.
[3] L.D. Nghiem, A.I. Schäfer, M. Elimelech, Nanofiltration of hormone mimicking trace organic contaminants, Sep. Sci. Technol., 40 (2005) 2633-2649.
[4] A.R.D. Verliefde, E.R. Cornelissen, S.G.J. Heijman, E.M.V. Hoek, G.L. Amy, B.V.d. Bruggen, J.C. van Dijk, Influence of solute-membrane affinity on rejection of uncharged organic solutes by nanofiltration membranes, Environ. Sci. Technol., 43 (2009) 2400-2406.
[5] A.J.C. Semião, A.I. Schäfer, Estrogenic micropollutant adsorption dynamics onto nanofiltration membranes, J. Membr. Sci., 381 (2011) 132-141.
[6] A.I. Schäfer, I. Akanyeti, A.J.C. Semião, Micropollutant sorption to membrane polymers: a review of mechanisms for estrogens, Adv Colloid Interfac, 164 (2011) 100-117.
[7] K. Kimura, S. Toshima, G. Amy, Y. Watanabe, Rejection of neutral endocrine disrupting compounds (EDCs) and pharmaceutical active compounds (PhACs) by RO membranes, J. Membr. Sci., 245 (2004) 71-78.
[8] S. Chang, T.D. Waite, A.I. Schäfer, A.G. Fane, Adsorption of the endocrine-active compound estrone on microfiltration hollow fiber membranes, Environ. Sci. Technol., 37 (2003) 3158-3163.
[9] Y. Yoon, P. Westerhoff, J. Yoon, S.A. Snyder, Removal of 17 beta Estradiol and Fluoranthene by Nanofiltration and Ultrafiltration, J. Environ. Eng., 130 (2004) 1460-1467.
[10] L.D. Nghiem, A.I. Schäfer, M. Elimelech, Role of electrostatic interactions in the retention of pharmaceutically active contaminants by a loose nanofiltration membrane, J. Membr. Sci., 286 (2006) 52-59.
[11] K. Boussu, C. Vandecasteele, B. Van der Bruggen, Relation between membrane characteristics and performance in nanofiltration, J. Membr. Sci., 310 (2008) 51-65.
[12] L.D. Nghiem, A.I. Schäfer, Adsorption and transport of trace contaminant estrone in NF/RO membranes, Environ. Eng. Sci., 19 (2002) 441-451.
[13] M.E. Williams, J.A. Hestekin, C.N. Smothers, D. Bhattacharyya, Separation of organic pollutants by reverse osmosis and nanofiltration membranes: mathematical models and experimental verification, Ind. Eng. Chem. Res., 38 (1999) 3683-3695.
[14] E. Steinle-Darling, E. Litwiller, M. Reinhard, Effects of sorption on the rejection of trace organic contaminants during nanofiltration, Environ. Sci. Technol., 44 (2010) 2592-2598.
[15] E.A. McCallum, H. Hyung, T.A. Do, C.-H. Huang, J.-H. Kim, Adsorption, desorption, and steady-state removal of 17β-estradiol by nanofiltration membranes, J. Membr. Sci., 319 (2008) 38-43.
[16] B. Van der Bruggen, J. Schaep, D. Wilms, C. Vandecasteele, Influence of molecular size, polarity and charge on the retention of organic molecules by nanofiltration, J. Membr. Sci., 156 (1999) 29-41.
[17] L.D. Nghiem, A.I. Schäfer, M. Elimelech, Removal of natural hormones by nanofiltration membranes: measurement, modeling, and mechanisms, Environ. Sci. Technol., 38 (2004) 1888-1896.
[18] E. Steinle-Darling, M. Reinhard, Nanofiltration for trace organic contaminant removal: structure, solution, and membrane fouling effects on the rejection of perfluorochemicals, Environ. Sci. Technol., 42 (2008) 5292-5297.
[19] J.Y. Hu, X. Jin, S.L. Ong, Rejection of estrone by nanofiltration: influence of solution chemistry, J. Membr. Sci., 302 (2007) 188-196.
[20] K. Kimura, G. Amy, J. Drewes, Y. Watanabe, Adsorption of hydrophobic compounds onto NF/RO membranes: an artifact leading to overestimation of rejection, J. Membr. Sci., 221 (2003) 89-101.

[21] C.Y. Tang, Y.-N. Kwon, J.O. Leckie, Probing the nano- and micro-scales of reverse osmosis membranes - a comprehensive characterization of physiochemical properties of uncoated and coated membranes by XPS, TEM, ATR-FTIR, and streaming potential measurements, J. Membr. Sci., 287 (2007) 146-156.
[22] A. Simon, L.D. Nghiem, P. Le-Clech, S.J. Khan, J.E. Drewes, Effects of membrane degradation on the removal of pharmaceutically active compounds (PhACs) by NF/RO filtration processes, J. Membr. Sci., 340 (2009) 16-25.
[23] J.O. Abitoye, P. Mukherjee, K. Jones, Ion implantation: effect on flux and rejection properties of NF membranes Environ. Sci. Technol., 39 (2005) 6487-6493.
[24] V. Freger, Swelling and morphology of the skin layer of polyamide composite membranes: an atomic force microscopy study, Environ. Sci. Technol., 38 (2004) 3168-3175.
[25] K. Boussu, J.D. Baerdemaeker, C. Dauwe, M. Weber, K. G. Lynn, D. Depla, S. Aldea, I. F. J. Vankelecom, V. Carlo, B.V.d. Bruggen, Physico-chemical characterization of nanofiltration membranes, ChemPhysChem, 8 (2007) 370-379.
[26] A.J.C. Semião, Removal of Adsorbing Estrogenic Micropollutants by Nanofiltration Membranes in Cross-Flow - Experiments and Model Development, in: Institute for Infrastructure and Environment, University of Edinburgh, 2011.
[27] A. De Munari, A.I. Schäfer, Impact of speciation on removal of manganese and organic matter by nanofiltration, J. Water Supply Res. Technol. AQUA, 59 (2010) 152-162.
[28] E. Bormashenko, R. Pogreb, G. Whyman, Y. Bormashenko, R. Jager, T. Stein, A. Schechter, D. Aurbach, The reversible giant change in the contact angle on the polysulfone and polyethersulfone films exposed to UV irradiation, Langmuir, 24 (2009) 5977-5980.
[29] A.H. Ellison, W.A. Zisman, Wettability studies on nylon, polyethylene terephthalate and polystyrene, J. Phys. Chem., 58 (1954) 503-506.
[30] A. Fujinami, D. Matsunaka, Y. Shibutani, Water wettability/non-wettability of polymer materials by molecular orbital studies, POLYMER, 50 (2009) 716-720.
[31] R.P. Schwarzenbach, P.M. Gschwend, D.M. Imboden, Environmental Organic Chemistry, 2nd Edition ed., Wiley-Interscience, 2003.
[32] L. Ji, W. Chen, S. Zheng, Z. Xu, D. Zhu, Adsorption of sulfonamide antibiotics to multiwalled carbon nanotubes, Langmuir, 25 (2009) 11608-11613.
[33] G.M. Loudon, Organic Chemistry, 2nd Edition ed., The Benjamin/Cummings Publishing Company, Inc., 1988.
[34] J.W. Steed, J.L. Atwood, Supramolecular chemistry, 2nd Edition ed., Wiley, 2009.
[35] L.D. Nghiem, Removal of emerging trace organic contaminants by nanofiltration and reverse osmosis, in: Faculty of Engineering, School of Civil, Mining, and Environmental Engineering, University of Wollongong, Wollongong, 2005, pp. 214.
[36] F.A. Pacheco, I. Pinnau, M. Reinhard, J.O. Leckie, Characterization of isolated polyamide thin films of RO and NF membranes using novel TEM techniques, J. Membr. Sci., 358 (2010) 51-59.
[37] P.S. Singh, S.V. Joshi, J.J. Trivedi, C.V. Devmurari, A.P. Rao, P.K. Ghosh, Probing the structural variations of thin film composite RO membranes obtained by coating polyamide over polysulfone membranes of different pore dimensions, J. Membr. Sci., 278 (2006) 19-25.
[38] A.K. Ghosh, E.M.V. Hoek, Impacts of support membrane structure and chemistry on polyamide–polysulfone interfacial composite membranes, J. Membr. Sci., 336 (2009) 140-148.
[39] W.R. Bowen, A.W. Mohammad, N. Hilal, Characterisation of nanofiltration membranes for predictive purposes - use of salts, uncharged solutes and atomic force microscopy, J. Membr. Sci., 126 (1997) 91-105.
[40] C. Combe, C. Guizard, P. Aimar, V. Sanchez, Experimental determination of four characteristics used to predict the retention of a ceramic nanofiltration membrane, J. Membr. Sci., 129 (1997) 147-160.
[41] W.M. Deen, Hindered transport of large molecules in liquid-filled pores, AlChE J., 33 (1987) 1409-1425.
[42] D.W. Green, R.H. Perry, Perry's Chemical Engineers' Handbook

8th ed., 2007.
[43] E. Worch, Eine neue Gleichung zur Berechnung von Diffusionskoeffizienten gelöster Stoffe, vom Wasser, 81 (1993) 289-297.
[44] H. Uedaira, H. Uedaira, Sugar-water interaction from diffusion measurements, J. Solution Chem., 14 (1985) 27-34.
[45] E.M. Renkin, Filtration, diffusion, and molecular sieving through porous cellulose membranes, J. Gen. Physiol., 38 (1954) 225-243.
[46] I. Sutzkover, D. Hasson, R. Semiat, Simple technique for measuring the concentration polarization level in a reverse osmosis system, Desalination, 131 (2000) 117-127.
[47] M.J. Rosa, M.N. de Pinho, Separation of organic solutes by membrane pressure-driven processes, J. Membr. Sci., 89 (1994) 235-243.
[48] V. Gekas, B. Hallström, Mass transfer in the membrane concentration polarization layer under turbulent cross flow : I. Critical literature review and adaptation of existing sherwood correlations to membrane operations, J. Membr. Sci., 30 (1987) 153-170.
[49] J. Schaep, C. Vandecasteele, A.W. Mohammad, W.R. Bowen, Analysis of the Salt Retention of Nanofiltration Membranes Using the Donnan–Steric Partitioning Pore Model, Sep. Sci. Technol., 34 (1999) 3009-3030.
[50] K. Kosutic, L. Kastelan-Kunst, B. Kunst, Porosity of some commercial reverse osmosis and nanofiltration polyamide thin-film composite membranes, J. Membr. Sci., 168 (2000) 101-108.
[51] M.N. de Pinho, V. Semião, V. Geraldes, Integrated modeling of transport processes in fluid/nanofiltration membrane systems, J. Membr. Sci., 206 (2002) 189-200.
[52] W.R. Bowen, J.S. Welfoot, Modelling the performance of membrane nanofiltration - critical assessment and model development, Chem. Eng. Sci., 57 (2002) 1121-1137.
[53] S.-Y. Kwak, D. Woo Ihm, Use of atomic force microscopy and solid-state NMR spectroscopy to characterize structure-property-performance correlation in high-flux reverse osmosis (RO) membranes, J. Membr. Sci., 158 (1999) 143-153.
[54] A.I. Schäfer, L.D. Nghiem, T.D. Waite, Removal of the natural hormone estrone from aqueous solutions using nanofiltration and reverse osmosis, Environ. Sci. Technol., 37 (2003) 182-188.
[55] A. Ben-David, S. Bason, J. Jopp, Y. Oren, V. Freger, Partitioning of organic solutes between water and polyamide layer of RO and NF membranes: correlation to rejection, J. Membr. Sci., 281 (2006) 480-490.

Table 1 Membrane characteristics

Membrane Type	Permeability ($L.h^{-1}.m^{-2}.bar^{-1}$)	NaCl Retention (%) (0.1 M, 10 bar)	Roughness R_A (nm)	Average Active Layer Thickness (nm)	Average Active Layer Thickness in Literature (nm)
BW30	4.1 ± 0.3	99.8	67.7 ± 2.4	233 ± 88 [21]	-
NF90	10.6 ± 1.6	88.7	61.7 ± 2.1	218 ± 40	[23]
TFC-SR2 1	12.5± 2.3	22.3	17.9 ± 0.6	345 ± 28	-
TFC-SR2 2	7.2 ± 0.6	23.4	17.9 ± 0.6	345 ± 28	-
TFC-SR3	6.7 ± 0.8	40.8	5.2 ± 0.6	400 ± 10	-
NF 270	17.0 ± 0.8	52.0	4.2 ± 0.3	21 ± 2.4	[24, 25]

Table 2 Polymer type, abbreviation (Abbr.), supplier, and selected characteristics for polymer powders used in adsorption studies: monomer molecular weight (MW) and contact angle (CA)

Polymer	Abbr.	Supplier	Structure	Monomer MW (g/mol)	CA (º)
Polysulphone	PSu	Solvay	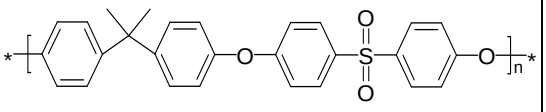	442	84 [28]
Polyester: Polyethylene Teraphthalate	PET	Goodfellow	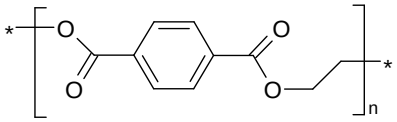	192	81 [29]
Polyester: Polyethylene Naphthalate	PEN	Goodfellow	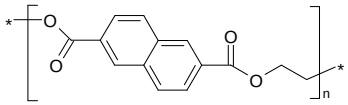	242	80 [30]
Polyamide: Nylon, 6	PA	Goodfellow	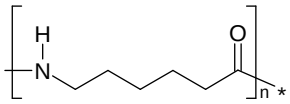	113	70 [29]

Table 3 Freundlich isotherm coefficients

Polymers	R^2	$1/n_i$	K_f
PA	0.99	1.5	$3.5.10^{-4}$
PSu	0.97	2.7	$7.6.10^{-12}$
PET	0.99	2.8	$1.0.10^{-12}$
PEN	0.99	3.4	$1.8.10^{-15}$

Table 4 Comparison between E2 diffusion cell adsorption and the polymer Freundlich isotherm

Diffusion Cell Conc (ng/L)	C equil (ng/L)	PA_m Mads (ng/cm^2)	C equil (ng/L)	PSu_m Mads (ng/cm^2)
100	80	6.12E-01	95	2.04E-01
30	24	1.63E-01	29	4.08E-03

Freundlich isotherm Conc (ng/L)	C equil (ng/L)	PA Mads (ng/cm^2)	C equil (ng/L)	PSu Mads (ng/cm^2)
100	80	7.92E-01	95	2.09E-02
30	24	1.30E-01	29	8.50E-04

Table 5 Organics characteristics

Organics	MW ($g.mol^{-1}$)	D_∞ ($m^2.s^{-1}$)	r_s (nm)
methanol	32	$1.81.10^{-9}$ [43]	0.13
dioxane	88.11	$9.82.10^{-10}$ [42]	0.24
xylose	150.13	$7.50.10^{-10}$ [44]	0.31
dextrose	180.16	$6.80.10^{-10}$ [45]	0.34

Table 6 Membrane pore radius (r_p) and thickness/porosity (δ/ε) ratio determination. The membrane active layer thickness is given in Table 1

Membranes	Average Pore Radius r_p (nm)	Active Layer Thickness Porosity Ratio δ/ε (μm)	Effective Interfacial Area of Active Layer A_{total} (cm^2)	Porosity
BW30	0.32 ± 0.01	5.4 ± 1.5	2953 ± 1776	0.04 ± 0.02
NF90	0.34 ± 0.04	0.8 ± 0.2	15439 ± 6700	0.26 ± 0.08
TFC-SR2 2	0.52 ± 0.03	2.5 ± 0.1	8501 ± 1497	0.14 ± 0.01
TFC-SR2 1	0.46 ± 0.01	1.1 ± 0.1	21461 ± 3191	0.32 ± 0.03
TFC-SR3	0.38 ± 0.01	1.60 ± 0.04	23817 ± 1728	0.25 ± 0.01
NF 270	0.42 ± 0.02	1.10 ± 0.04	134 ± 18	0.020 ± 0.002

Table 7 Comparison between the experimental and Hagen-Poiseullie permeabilities

Membrane	**Experimental Permeability (m/s)**	**H-P permeability (m/s)**
BW30	1.25×10^{-5}	2.81×10^{-6}
NF90	3.24×10^{-5}	2.05×10^{-5}
TFC-SR2 2	3.82×10^{-5}	1.63×10^{-5}
TFC-SR2 1	2.20×10^{-5}	2.86×10^{-5}
TFC-SR3	2.05×10^{-5}	1.33×10^{-5}
NF270	5.19×10^{-5}	2.36×10^{-5}

List of Figures

Figure 8 Estradiol (E2) mass adsorbed per cross-flow surface area (Mass Ads.) ($ng.cm^{-2}$) and membrane effective interfacial area A_{total} (cm^2) with increasing effective pore radius (Table 6) (Cross-flow conditions: C_{feed} initial=100 $ng.L^{-1}$, 24°C, 11 bar, Re_h=1450, pH 7). The variability in A_{total} is presented as error bar.

Figure 9 Estradiol (E2) mass adsorbed per cross-flow surface area (Mass Ads.) for the NF90 and the TFC-SR2 2 membrane for pH 7 and 11. (Cross-flow conditions: C_{feed} initial=100 $ng.L^{-1}$, Re_h=1450, 11 bar, 24°C)

Figure 10 Estrone (E1) mass adsorbed extracted (%) from the NF270 membrane for different pressures used to saturate the membranes (filtered extraction in cross-flow: T=24ºC, Re_h=427, P=11 bar, MilliQ water, then MilliQ+acetone solution (2%); static desorption: T=24ºC, 200 rpm, acetone). Triplicates of selected experiments were carried out and it was found that the variability in hormone extraction was of ± 8.5% for filtration experiments

Figure 11 Conceptual schematic of the effect of (A) internal surface area (*i.e.* active layer thickness δ) and (B) pore radius r_p in hormone adsorption in the active layer